Bright-Exciton Fine-Structure Splittings in Single Perovskite Nanocrystals

Chunyang Yin,[1] Liyang Chen,[1] Nan Song,[1] Yan Lv,[1] Fengrui Hu,[1] Chun Sun,[2] William W. Yu,[2] Chunfeng Zhang,[1] Xiaoyong Wang,[1,*] Yu Zhang,[2,†] and Min Xiao[1,3,‡]

[1]*National Laboratory of Solid State Microstructures, School of Physics, and Collaborative Innovation Center of Advanced Microstructures, Nanjing University, Nanjing 210093, China*

[2]*State Key Laboratory on Integrated Optoelectronics and College of Electronic Science and Engineering, Jilin University, Changchun 130012, China*

[3]*Department of Physics, University of Arkansas, Fayetteville, Arkansas 72701, USA*

(Received 8 January 2017; revised manuscript received 14 May 2017; published 11 July 2017)

Here we show that, in single perovskite $CsPbI_3$ nanocrystals synthesized from a colloidal approach, a bright-exciton fine-structure splitting as large as hundreds of μeV can be resolved with two orthogonally and linearly polarized photoluminescence peaks. This doublet could switch to a single peak when a single $CsPbI_3$ nanocrystal is photocharged to eliminate the electron-hole exchange interaction. The above findings have prepared an efficient platform suitable for probing exciton and spin dynamics of semiconductor nanostructures at the visible-wavelength range, from which a variety of practical applications such as in entangled photon-pair source and quantum information processing can be envisioned.

DOI: 10.1103/PhysRevLett.119.026401

The electron-hole exchange interaction (*e-h* EI) is greatly enhanced in quantum-confined semiconductor nanostructures, leading to the energy-level splitting between bright- and dark-exciton states [1,2]. In semiconductor epitaxial quantum dots (QDs), the dark excitons are generally nonemissive without applying a magnetic field [3] and the bright-exciton state is further divided into two orthogonally and linearly polarized ones [4]. The existence of such a bright-exciton fine-structure splitting (FSS) has been positively employed to generate a target wave function from coherent superposition of the two constituent states [5] and to develop a two-bit conditional quantum logic in the two-exciton configuration [6]. Meanwhile, complete elimination of this bright-exciton FSS has been actively pursued to realize a polarization-entangled photon-pair source [7–10] for fundamental tests in quantum mechanics and optics [11], as well as for practical applications in quantum communication [12–14]. Interestingly, the dark excitons in colloidal semiconductor nanocrystals (NCs) are rendered emissive due to spin-mixing interactions with several proposed sources [2,15–17], and the exciton FSS in this case usually refers to their energy separation from that of bright excitons [18,19] whose doublet states were rarely resolved. Even in the few limited reports on single CdSe NCs [20,21], the random orientation of their crystallographic axis, together with the photoluminescence (PL) blinking and spectral diffusion effects, posed severe obstacles to investigating the polarized bright-exciton FSS so that its existence is still questionable [22].

Colloidal perovskite NCs have just emerged as a new type of semiconductor nanostructure [23–25] capable of emitting single photons without the influence of dark-exciton emission [26–28]. Moreover, the suppressions of both the PL blinking and spectral diffusion effects were successfully demonstrated in single perovskite $CsPbI_3$ NCs [29]. Here we show that the bright-exciton FSS can be easily observed in single $CsPbI_3$ NCs at the cryogenic temperature, with an energy separation as large as hundreds of μeV between the two orthogonally and linearly polarized states. With the laser excitation at an intermediate power, this PL doublet of neutral single exciton (X) would switch to a single peak of singly charged single exciton (X^-). When the laser power is further increased, PL doublets from neutral biexciton (XX), charged biexciton (XX^-), and doubly charged single exciton (X^{2-}) could be additionally observed. Based on the FSS values obtained from various exciton species, the isotropic and anisotropic *e-h* EI energies can be roughly estimated, which has provided valuable information on the fundamental electronic processes in these novel perovskite NCs.

According to the same methods as reported previously [29], the perovskite $CsPbI_3$ NCs studied here were colloidally synthesized with a cubic size of ~9.3 nm, and all the optical characterizations of single $CsPbI_3$ NCs were performed at the cryogenic temperature of ~4 K (see experimental details in the Supplemental Material [30]). The 570 nm output of a 5.6 MHz picosecond fiber laser was used as the excitation source and its output power could be adjusted to tune the number of excitons (N) created per pulse in a single NC (see Fig. S1 in the Supplemental Material [30] for the estimation of N). In Fig. 1(a), we plot the PL spectra collected, respectively, at 0° (red), 45° (black), and 90° (blue) for a representative $CsPbI_3$ NC excited at $N = \sim 0.05$, where the 0° corresponded to the angle of the polarizer set before the spectrometer to get a maximum PL intensity from the higher energy peak of the observed PL doublet. The possibility that more than one NC contributed to this orthogonally and linearly polarized PL doublet was safely ruled out from the second-order photon correlation measurement that yielded a $g^2(\tau)$ value

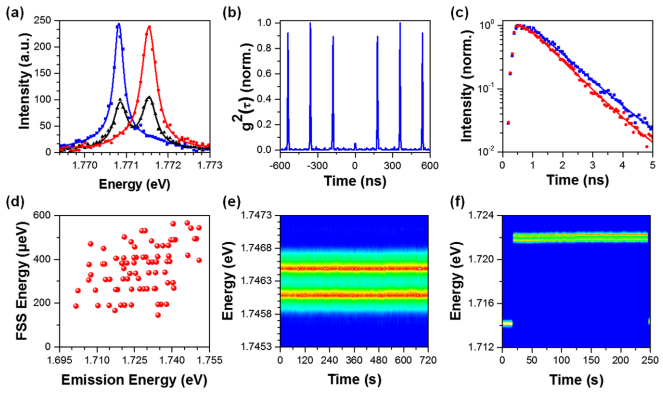

FIG. 1. (a) PL spectra of a single $CsPbI_3$ NC measured at the polarization angles of 0° (red), 45° (black), and 90° (blue), respectively. The PL data points are fitted by Lorentzian functions. (b) Second-order photon correlation measurement for this single $CsPbI_3$ NC at the polarization angle of 45°. (c) PL decay curves measured for the higher (red) and lower (blue) energy peaks of this single $CsPbI_3$ NC at the polarization angles of 0° and 90°, respectively, and fitted with single-exponential functions. (d) Statistical distribution of the FSS energies plotted for ~80 single $CsPbI_3$ NCs as a function of their emission energies of the higher energy components of the doublet transitions. The small range covered by the emission energies of single $CsPbI_3$ NCs can be attributed mainly to their narrow size distribution. (e) Time-dependent PL spectral image of a single $CsPbI_3$ NC showing the long-time stability of the FSS. (f) Time-dependent PL spectral image of a single $CsPbI_3$ NC with the appearances of both X and X^- peaks. The laser excitation power for the optical measurements in (a)–(e) corresponded to $N = \sim 0.05$, while that in (f) corresponded to $N = \sim 0.8$. The integration time for acquiring the PL spectra in (a) [(e) and (f)] was 5 s [1 s]. The PL measurements in (e) and (f) were performed without any polarization selection. In (a), a.u. denotes arbitrary units.

of ~0.05 at the zero time delay and the polarization angle of 45° [Fig. 1(b)]. As shown in Fig. 1(c), the PL decay curves measured for the higher (red) and lower (blue) energy peaks could both be fitted with single-exponential lifetimes of ~0.93 and ~1.02 ns, respectively, thus confirming their bright-exciton nature of the optical emission. With a spectral resolution of ~200 μeV in the PL measurements, we plot in Fig. 1(d) a statistical distribution of the FSS values measured for ~80 single $CsPbI_3$ NCs as a function of their emission energies of the higher energy components of the doublet transitions, from which an average value of 356 ± 108 μeV could be obtained.

In our previous report [29], most of the studied $CsPbI_3$ NCs had a single PL peak with a linewidth close to ~200 μeV and only ~10% of them possessed relatively broader peaks with the PL doublets being not clearly resolved. Although the same synthesis procedure was nominally adopted, almost 80% of the total $CsPbI_3$ NCs studied here demonstrated an obvious FSS effect, implying that it is very sensitive to some trivial conditions that are too difficult to be actively controlled right now. In semiconductor epitaxial QDs, the bright-exciton FSSs from tens to hundreds of μeV are normally caused by the QD anisotropies in shape and strain [1]. The above two factors can be largely ruled out in perovskite $CsPbI_3$ NCs since they are associated with an almost symmetric shape from the TEM measurement [29], and the apparent lack of the size-dependent FSSs in Fig. 1(d) excludes the participation of strain-induced piezoelectric fields that should be monotonically influenced by the size or volume [31]. Since the crystal structures are intimately related to the FSSs in epitaxial QDs [32,33], we speculate that it might be the lattice anisotropy, amenable to possible influences in each synthesis process, that contributes to the large FSSs observed here in single $CsPbI_3$ NCs. Recently, a PL anisotropy as large as ~40% was observed from a solid film of ensemble $CsPbI_3$ NCs, while it completely disappeared in the case of $CsPbBr_3$ NCs [34]. It was proposed that the replacement of bromide by bigger iodine atoms would distort the cubic structure to break the space inversion symmetry, resulting in anisotropic dipole moments along the three crystal directions [34]. Although the exact origins are yet to be investigated both theoretically and experimentally in future works, it does not hinder us at the current stage to explore the fundamental properties of this intriguing FSS effect in perovskite $CsPbI_3$ NCs.

These PL doublets are very robust against the measurement time, as can be seen in Fig. 1(e) from the time-dependent PL spectral image of a representative $CsPbI_3$ NC also excited at $N = \sim 0.05$. When the laser power was increased to make $N > \sim 0.5$, a PL doublet would switch occasionally to a redshifted peak [see Fig. 1(f) and Figs. S2(a) and S2(b) in the Supplemental Material [30]]. Similar to the case of colloidal CdSe NCs [35], this new spectral feature observed here in single perovskite NCs was previously attributed to the optical emission from X^- [29] (see the Supplemental Material [30] for discussions on the sign of charged excitons), whose total electron spin is zero so that the e-h EI vanishes to render a single PL peak without the FSS [31,36]. In previous optical studies of single perovskite NCs [28,29], both the X and X^- peaks existed within a given integration time due to the extremely fast charging and decharging events. In great contrast, the PL spectrum of X^- studied here in single $CsPbI_3$ NCs could be well separated from that of X in the time domain and even lasted for tens of minutes once N was decreased to ~0.1 after it was triggered at higher laser powers [see Fig. S2(c) in the Supplemental Material [30]]. Because the X^- state can be treated as a pure two-level system with a well-defined spin [37], its easy access and long-time stability shown here in single $CsPbI_3$ NCs highlight their great potentials in quantum technology applications such as spin storage, manipulation, and readout [38].

When the laser excitation power was further increased, optical emissions from more complex exciton species could be observed in single $CsPbI_3$ NCs, which are the hallmarks of their greatly reduced Auger recombination processes. In Fig. 2(a), we plot the time-dependent PL spectral image of a

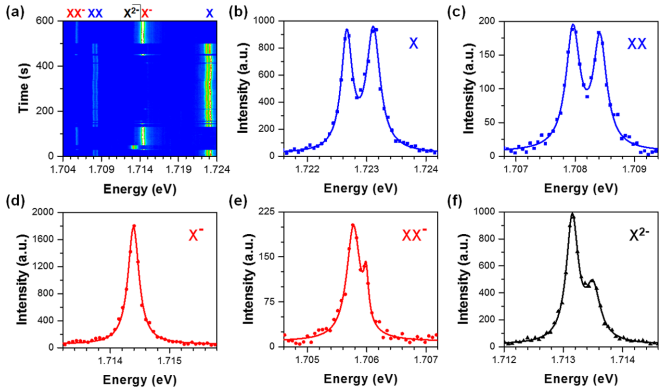

FIG. 2. (a) Time-dependent PL spectral image of a single $CsPbI_3$ NC excited at $N = \sim 1.5$ with the appearances of various exciton species marked on the top by XX^-, XX, X^{2-}, X^-, and X, respectively. The PL spectra of X, XX, X^-, XX^-, and X^{2-} are plotted in (b)–(f), respectively. The PL data points of X^- are fitted with a single Lorentzian function, while those of other exciton species are fitted with the summations of two Lorentzian functions. The integration time for all the above PL measurements was 1 s. All of the above PL measurements were performed without any polarization selection. In (b)-(f), a.u. denotes arbitrary units.

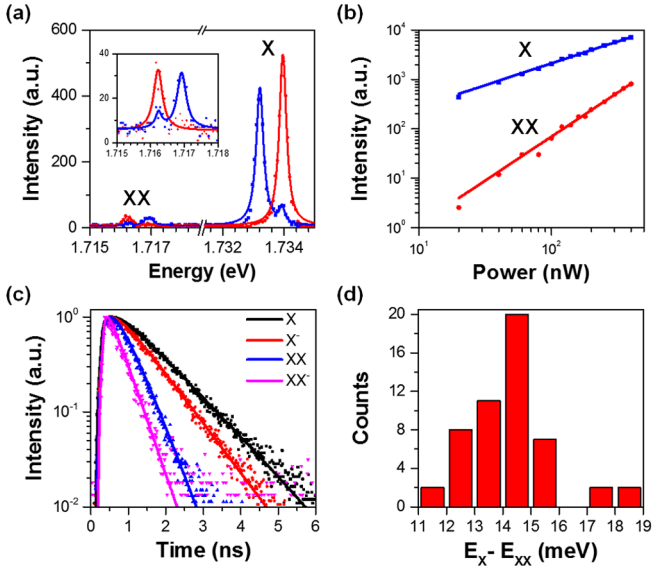

FIG. 3. (a) PL spectra measured at the polarization angles of 0° (red) and 90° (blue) for X and XX of a single $CsPbI_3$ NC excited at $N = \sim 1.5$. Inset: An enlarged view of the XX PL spectra. (b) PL intensities of X and XX of this single $CsPbI_3$ NC plotted as a function of the laser excitation power with fitting slopes of ~0.89 and ~1.78, respectively. (c) PL decay curves obtained at $N = \sim 1.5$ for X, X^-, XX, and XX^- of this single $CsPbI_3$ NC and fitted with single-exponential functions. (d) Statistical distribution of the XX binding energies measured for ~50 single $CsPbI_3$ NCs with an average value of $\sim 14.26 \pm 1.53$ meV. The XX binding energy was calculated between the average energies of the X and the XX PL doublets. The integration time for the PL measurements in (a) and (b) was 1 s. In (a)-(c), a.u. denotes arbitrary units.

representative $CsPbI_3$ NC excited at $N = \sim 1.5$. Since the PL peak from X (X^-) has already been defined in Fig. 1(f) for this single NC excited at $N = \sim 0.8$, the accompanying one emitted at a longer wavelength can be safely attributed to the optical emission from XX (XX^-). We tentatively assign an additional PL peak, redshifted only a little bit relative to that of X^-, to the optical emission from X^{2-} due to the addition of an extra electron to the X^- configuration. Corresponding to Fig. 2(a), the PL spectra of X, XX, X^-, XX^-, and X^{2-} are sequentially plotted in Figs. 2(b)–(f) (see Fig. S3 in the Supplemental Material [30] for a full PL spectrum of this single NC), where the emergence of FSSs in XX and XX^- is naturally expected according to previous optical studies of single epitaxial QDs [8–10,39,40]. In Figs. S4 and S5 of the Supplemental Material [30], we demonstrate similar results from four more $CsPbI_3$ NCs to justify the universal appearance of all the above exciton species.

Next, we will elaborate more on the optical properties of XX since its existence is a prerequisite for the realization of entangled photon pairs by means of electrical [41], optical [42], magnetic [3], or piezoelectric [43] tuning of the X FSSs. In Fig. 3(a), we plot the PL spectra of a representative $CsPbI_3$ NC excited at $N = \sim 1.5$, with two sets of orthogonally and linearly polarized PL doublets originating from X and XX, respectively (see the inset for an enlarged view of the XX peaks). The higher (lower) energy X and the lower (higher) energy XX peaks have the same linear polarization because the two cascading channels, each from XX to the ground state with X being an intermediate state, should conserve the same total energy [3,41–43]. As shown in Fig. 3(b), the X and XX PL intensities have linear and quadratic dependences on the laser excitation power, respectively, thus confirming again the correctness of their respective origins [44]. Similar dependences of the X^- and XX^- PL intensities on the laser excitation powers are shown in Fig. S6 of the Supplemental Material [30]. In Fig. 3(c), we plot the PL decay curves measured for various exciton species for this specific $CsPbI_3$ NC, whose single-exponential fittings yielded the PL lifetimes of ~1.07, ~0.83, ~0.41, and ~0.36 ns for X, X^-, XX, and XX^-, respectively (see Fig. S7 in the Supplemental Material [30] for similar PL decay curves measured for three other representative $CsPbI_3$ NCs). Because the PL lifetime ratio of ~2.61 between X and XX is larger than the expected value of 2 [45,46] and the PL intensity of XX is several times lower than that of X even at the highest excitation power in our experiment [Fig. 3(b)], we speculate that nonradiative Auger recombination might still contribute to the XX decay process. From statistical measurements of ~50 single $CsPbI_3$ NCs for the energy differences between X and XX [Fig. 3(d)], the average binding energy of XX was calculated to be $\sim 14.26 \pm 1.53$ meV, which is relatively larger than those of $\sim 7.61 \pm 1.43$, $\sim 8.78 \pm 1.08$, and $\sim 2.19 \pm 0.63$ meV obtained for X^-, XX^-, and X^{2-}, respectively (see Fig. S8 in the Supplemental Material [30]). As shown in Fig. S9 of the Supplemental Material [30], the X FSS value increases slightly with the increasing XX binding energy, which implies

TABLE I. Electron-hole EI energies of five representative $CsPbI_3$ NCs. Δ_0^2, Δ_0^1, and Δ_1^1 denote, respectively, the isotropic $2e^1$-$1h^1$, the isotropic $1e^1$-$1h^1$, and the anisotropic $1e^1$-$1h^1$ EI energies in the unit of μeV.

NC no.	Δ_0^2	Δ_0^1	Δ_1^1	Δ_1^1/Δ_0^1
I	350	214	448	2.093
II	304	319	372	1.166
III	348	282	442	1.567
IV	337	273	264	0.967
V	382	356	201	0.565

that the overlap of e-h wave functions and the anisotropy in NC composition may also play a role in the e-h EI [47].

The origin of the PL doublet in Fig. 2(f) from X^{2-} can be strongly corroborated by the fact that it starts from and ends into the X^- PL peak in a time-dependent PL spectral measurement (see Fig. S10 in the Supplemental Material [30]), which can be plausibly explained by the acquirement and release of an extra electron in the perovskite $CsPbI_3$ NC. Moreover, the PL intensity of the lower energy peak is about twice that of the higher energy one, which can be similarly found in other single $CsPbI_3$ NCs (see Figs. S4 and S5 in the Supplemental Material [30]). This fixed PL intensity ratio of X^{2-} has been well explained in previous optical studies of single epitaxial QDs involving FSSs in the initial and final recombination states [32,40,48,49] (see the schematics of Fig. S11 and related discussions in the Supplemental Material [30]). The FSS of X^{2-}, together with those of X and XX^-, can provide valuable information on the degrees of various e-h EIs in perovskite $CsPbI_3$ NCs. The FSS of XX^- is equal to the isotropic $1e^1$-$1h^1$ EI energy (Δ_0^1) and that of X to the anisotropic $1e^1$-$1h^1$ EI energy (Δ_1^1) [39,50]. The FSS of X^{2-} gives the isotropic $2e^1$-$1h^1$ EI energy (Δ_0^2), while its anisotropic $2e^1$-$1h^1$ EI energies (Δ_1^2 and Δ_2^2) can be generally neglected (see Refs. [32,40], as well as the Supplemental Material [30] for further discussions). In the above notations ($1e^1$-$1h^1$ and $2e^1$-h^1), the number before and the superscript of e (h) denote the shell and the number of electrons (holes) participating in the EI interaction. As listed in Table I for five representative $CsPbI_3$ NCs, the average values of Δ_1^1 and Δ_0^2 are 345 ± 110 and 344 ± 28 μeV, respectively. The average value of Δ_0^1 is $\sim 290 \pm 50$ μeV, which is smaller than those of epitaxial CdSe/ZnSe ($\sim 1.6 \pm 0.1$ meV) [39,50] and InGaAs ($\sim$0.6 meV) [40] QDs, leading to a relatively larger ratio of $\sim 1.27 \pm 0.58$ for Δ_1^1/Δ_0^1 in $CsPbI_3$ NCs. In contrast, the Δ_1^1/Δ_0^1 ratio is $\sim$0.5 for CdSe/ZnSe QDs [39] and $\Delta_1^1 \ll \Delta_0^1$ in the case of InGaAs QDs [40], signifying again the important role played by lattice anisotropy [32] in the FSS of perovskite $CsPbI_3$ NCs.

To summarize, we have observed energy-level FSSs of various exciton species in single perovskite $CsPbI_3$ NCs, which are "atomiclike" features typically possessed only by epitaxial QDs. The above findings signify that perovskite NCs are equipped with a "hybrid" feature to bridge the long-missing gap between epitaxial QDs and colloidal NCs to get these two important semiconductor nanostructure systems coherently connected. Moreover, the intrinsic energy-level structures resolved here from perovskite NCs have not only brought them into the potential applications in quantum information processing but also provided valuable information on the basic electronic processes of their bulk (film) counterpart for optimal device performances. We are optimistic that abundant research opportunities exist in the bright-exciton FSS itself to stimulate great theoretical and experimental interests in perovskite NCs. Theoretically, the most challenging task is to set up a suitable model correlating the observed FSS values to specific origins. It is also necessary to determine the light- or heavy-hole nature of the band-edge excitons as well as their exact energy-level alignments. Experimentally, the electrical, magnetic, or optical field could be applied to a single perovskite NC to tune the bright-exciton FSS, the response of which will be analyzed not only to reveal its real underlying mechanism but also to seek the possibility of realizing entangled photon pairs at the visible-wavelength range. With the 5.6 MHz laser excitation at $N = \sim 1.0$, the single-photon detector counts could reach 6 kcounts per sec from the X emission of a single $CsPbI_3$ NC, which are close to the high counts of modern epitaxial QDs integrated into, e.g., a nanowire waveguide [51]. To make single perovskite NCs a potent nanostructure object in both fundamental studies and practical applications, it would be necessary to further increase the photon extraction efficiency by embedding them into various optical structures such as a dielectric antenna [52] and an open planar-concave cavity [53].

This work is supported by the National Key R&D Research Program of China (2017YFA0303700), the National Natural Science Foundation of China (Grants No. 11574147, No. 91321105, No. 11274161, and No. 11621091), the Fundamental Research Funds for the Central Universities (0204-14380052), and the PAPD of Jiangsu Higher Education Institutions.

*Corresponding author.
wxiaoyong@nju.edu.cn
†Corresponding author.
yuzhang@jlu.edu.cn
‡Corresponding author.
mxiao@uark.edu

[1] G. Bester, S. Nair, and A. Zunger, Phys. Rev. B **67**, 161306 (2003).
[2] M. Nirmal, D. J. Norris, M. Kuno, M. G. Bawendi, A. L. Efros, and M. Rosen, Phys. Rev. Lett. **75**, 3728 (1995).
[3] M. Bayer, A. Kuther, A. Forchel, A. Gorbunov, V. B. Timofeev, F. Schäfer, J. P. Reithmaier, T. L. Reinecke, and S. N. Walck, Phys. Rev. Lett. **82**, 1748 (1999).
[4] D. Gammon, E. S. Snow, B. V. Shanabrook, D. S. Katzer, and D. Park, Phys. Rev. Lett. **76**, 3005 (1996).
[5] N. H. Bonadeo, J. Erland, D. Gammon, D. Park, D. S. Katzer, and D. G. Steel, Science **282**, 1473 (1998).
[6] X. Li, Y. Wu, D. Steel, D. Gammon, T. H. Stievater, D. S. Katzer, D. Park, C. Piermarocchi, and L. J. Sham, Science **301**, 809 (2003).

[7] O. Benson, C. Santori, M. Pelton, and Y. Yamamoto, Phys. Rev. Lett. **84**, 2513 (2000).
[8] R. M. Stevenson, R. J. Young, P. Atkinson, K. Cooper, D. A. Ritchie, and A. J. Shields, Nature (London) **439**, 179 (2006).
[9] A. Dousse, J. Suffczyński, A. Beveratos, O. Krebs, A. Lemaître, I. Sagnes, J. Bloch, P. Voisin, and P. Senellart, Nature (London) **466**, 217 (2010).
[10] M. Muller, S. Bounouar, K. D. Jons, M. Glassl, and P. Michler, Nat. Photonics **8**, 224 (2014).
[11] A. Aspect, P. Grangier, and G. Roger, Phys. Rev. Lett. **49**, 91 (1982).
[12] D. Bouwmeester, J.-W. Pan, K. Mattle, M. Eibl, H. Weinfurter, and A. Zeilinger, Nature (London) **390**, 575 (1997).
[13] E. Knill, R. Laflamme, and G. J. Milburn, Nature (London) **409**, 46 (2001).
[14] N. Gisin, G. Ribordy, W. Tittel, and H. Zbinden, Rev. Mod. Phys. **74**, 145 (2002).
[15] S. A. Crooker, T. Barrick, J. A. Hollingsworth, and V. I. Klimov, Appl. Phys. Lett. **82**, 2793 (2003).
[16] O. Labeau, P. Tamarat, and B. Lounis, Phys. Rev. Lett. **90**, 257404 (2003).
[17] L. Biadala, Y. Louyer, P. Tamarat, and B. Lounis, Phys. Rev. Lett. **103**, 037404 (2009).
[18] M. J. Fernée, B. N. Littleton, and H. Rubinsztein-Dunlop, ACS Nano **3**, 3762 (2009).
[19] L. Biadala, Y. Louyer, P. Tamarat, and B. Lounis, Phys. Rev. Lett. **105**, 157402 (2010).
[20] M. Furis, H. Htoon, M. A. Petruska, V. I. Klimov, T. Barrick, and S. A. Crooker, Phys. Rev. B **73**, 241313 (2006).
[21] H. Htoon, M. Furis, S. A. Crooker, S. Jeong, and V. I. Klimov, Phys. Rev. B **77**, 035328 (2008).
[22] Y. Louyer, L. Biadala, P. Tamarat, and B. Lounis, Appl. Phys. Lett. **96**, 203111 (2010).
[23] L. Protesescu, S. Yakunin, M. I. Bodnarchuk, F. Krieg, R. Caputo, C. H. Hendon, R. X. Yang, A. Walsh, and M. V. Kovalenko, Nano Lett. **15**, 3692 (2015).
[24] F. Zhang, H. Zhong, C. Chen, X.-G. Wu, X. Hu, H. Huang, J. Han, B. Zou, and Y. Dong, ACS Nano **9**, 4533 (2015).
[25] N. S. Makarov, S. Guo, O. Isaienko, W. Liu, I. Robel, and V. I. Klimov, Nano Lett. **16**, 2349 (2016).
[26] Y.-S. Park, S. Guo, N. S. Makarov, and V. I. Klimov, ACS Nano **9**, 10386 (2015).
[27] F. Hu, H. Zhang, C. Sun, C. Yin, B. Lv, C. Zhang, W. W. Yu, X. Wang, Y. Zhang, and M. Xiao, ACS Nano **9**, 12410 (2015).
[28] G. Rainò, G. Nedelcu, L. Protesescu, M. I. Bodnarchuk, M. V. Kovalenko, R. F. Mahrt, and T. Stöferle, ACS Nano **10**, 2485 (2016).
[29] F. Hu, C. Yin, H. Zhang, C. Sun, W. W. Yu, C. Zhang, X. Wang, Y. Zhang, and M. Xiao, Nano Lett. **16**, 6425 (2016).
[30] See Supplemental Material at http://link.aps.org/supplemental/10.1103/PhysRevLett.119.026401 for the experimental details; the estimation for the number of excitons created per pulse in a single NC; PL spectra of X and X^- of a single NC, as well as the long-time stability of the X^- PL; PL spectra of various exciton species plotted together; the PL peaks of X, XX, X^-, XX^-, and X^{2-} of several single NCs; PL intensities of X^- and XX^- plotted as a function of the laser excitation powers; PL decay curves of X, X^-, XX, and XX^-; statistical distributions of the X^-, XX^-, and X^{2-} binding energies; statistical distribution of the X FSS values plotted as a function of the X and XX energy differences; time-dependent transitions between the optical emissions of X^- and X^{2-}; discussions on the sign of charged excitons; and discussions on the energy-level structures of X^{2-}.
[31] R. Seguin, A. Schliwa, S. Rodt, K. Pötschke, U. W. Pohl, and D. Bimberg, Phys. Rev. Lett. **95**, 257402 (2005).
[32] M. Ediger, G. Bester, B. D. Gerardot, A. Badolato, P. M. Petroff, K. Karrai, A. Zunger, and R. J. Warburton, Phys. Rev. Lett. **98**, 036808 (2007).
[33] L. He, M. Gong, C.-F. Li, G.-C. Guo, and A. Zunger, Phys. Rev. Lett. **101**, 157405 (2008).
[34] D. Wang, D. Wu, D. Dong, W. Chen, J. Hao, J. Qin, B. Xu, K. Wang, and X. Sun, Nanoscale **8**, 11565 (2016).
[35] C. Galland, Y. Ghosh, A. Steinbrück, J. A. Hollingsworth, H. Htoon, and V. I. Klimov, Nat. Commun. **3**, 908 (2012).
[36] A. Högele, S. Seidl, M. Kroner, K. Karrai, R. J. Warburton, B. D. Gerardot, and P. M. Petroff, Phys. Rev. Lett. **93**, 217401 (2004).
[37] S. Strauf, N. G. Stoltz, M. T. Rakher, L. A. Coldren, P. M. Petroff, and D. Bouwmeester, Nat. Photonics **1**, 704 (2007).
[38] M. Kroutvar, Y. Ducommun, D. Heiss, M. Bichler, D. Schuh, G. Abstreiter, and J. J. Finley, Nature (London) **432**, 81 (2004).
[39] I. A. Akimov, A. Hundt, T. Flissikowski, and F. Henneberger, Appl. Phys. Lett. **81**, 4730 (2002).
[40] B. Urbaszek, R. J. Warburton, K. Karrai, B. D. Gerardot, P. M. Petroff, and J. M. Garcia, Phys. Rev. Lett. **90**, 247403 (2003).
[41] M. Ghali, K. Ohtani, Y. Ohno, and H. Ohno, Nat. Commun. **3**, 661 (2012).
[42] A. Muller, W. Fang, J. Lawall, and G. S. Solomon, Phys. Rev. Lett. **103**, 217402 (2009).
[43] Y. Chen, J. Zhang, M. Zopf, K. Jung, Y. Zhang, R. Keil, F. Ding, and O. G. Schmidt, Nat. Commun. **7**, 10387 (2016).
[44] Y. Louyer, L. Biadala, J.-B. Trebbia, M. J. Fernée, P. Tamarat, and B. Lounis, Nano Lett. **11**, 4370 (2011).
[45] G. Bacher, R. Weigand, J. Seufert, V. D. Kulakovskii, N. A. Gippius, A. Forchel, K. Leonardi, and D. Hommel, Phys. Rev. Lett. **83**, 4417 (1999).
[46] Y.-S. Park, W. K. Bae, J. M. Pietryga, and V. I. Klimov, ACS Nano **8**, 7288 (2014).
[47] M. Ściesiek, J. Suffczyński, W. Pacuski, M. Parlińska-Wojtan, T. Smoleński, P. Kossacki, and A. Golnik, Phys. Rev. B **93**, 195313 (2016).
[48] T. Kazimierczuk, T. Smoleński, J. Kobak, M. Goryca, W. Pacuski, A. Golnik, K. Fronc, Ł. Kłopotowski, P. Wojnar, and P. Kossacki, Phys. Rev. B **87**, 195302 (2013).
[49] R. J. Warburton, C. Schäflein, D. Haft, F. Bickel, A. Lorke, K. Karrai, J. M. Garcia, W. Schoenfeld, and P. M. Petroff, Nature (London) **405**, 926 (2000).
[50] I. A. Akimov, K. V. Kavokin, A. Hundt, and F. Henneberger, Phys. Rev. B **71**, 075326 (2005).
[51] M. A. M. Versteegh, M. E. Reimer, K. D. Jöns, D. Dalacu, P. J. Poole, A. Gulinatti, A. Giudice, and V. Zwiller, Nat. Commun. **5**, 5298 (2014).
[52] K. G. Lee, X. W. Chen, H. Eghlidi, P. Kukura, R. Lettow, A. Renn, V. Sandoghdar, and S. Götzinger, Nat. Photonics **5**, 166 (2011).
[53] S. Dufferwiel, F. Fras, A. Trichet, P. M. Walker, F. Li, L. Giriunas, M. N. Makhonin, L. R. Wilson, J. M. Smith, E. Clarke, M. S. Skolnick, and D. N. Krizhanovskii, Appl. Phys. Lett. **104**, 192107 (2014).